Aromaticity

DOI: 10.1002/anie.201001765

Möbius Antiaromatic Bisphosphorus Complexes of [30]Hexaphyrins**

Tomohiro Higashino, Jong Min Lim, Takahiro Miura, Shohei Saito, Jae-Yoon Shin, Dongho Kim, and Atsuhiro Osuka**

Aromaticity is a fundamental concept in organic chemistry and is important in understanding, for instance, that the energetic stability of benzene originates from cyclic π-electron delocalization. The Hückel rule is very useful, and helps us to predict that cyclic $[4n+2]\pi$- and $[4n]\pi$-conjugated systems should be aromatic and antiaromatic, respectively, given that their π systems lie on two-sided normal planes. On the other hand, Möbius aromaticity, which complements the Hückel aromaticity, predicts that the above $[4n+2]$ and $[4n]$ Hückel rule should be reversed for those π systems that lie on a singly twisted Möbius topology.[1] The concept of Möbius aromaticity, first proposed by Heilbronner in 1964,[2] is simple and elegant, and has considerably stimulated both experimental and theoretical approaches toward Möbius aromatic molecules.[1b,c,3] However, the realization of Möbius aromatic systems is difficult, since the implementation of two conflicting structural features, that is, cyclic full π conjugation and a singly twisted topology, within a single macrocycle is not easy. Despite this difficulty, a seminal report by Herges and co-workers described the synthesis and moderate aromaticity of a twisted [16]annulene molecule.[4] Importantly, this work revitalized the interest in Möbius aromaticity. In recent years, meso-aryl-substituted expanded porphyrins have emerged as a remarkably effective platform to realize stable Möbius aromatic systems. The attributes of these porphyrins include conformational flexibility, which allows flipping of the constitutional pyrrole rings, and the availability of the neutral states for two-electron oxidation and reduction by releasing two protons from aminopyrrole parts and accepting two hydride ions at the iminopyrrolic parts, respectively.[5]

However, despite the increasing number of $[4n]\pi$ Möbius aromatic molecules, $[4n+2]\pi$ Möbius antiaromatic species still remain rather elusive. As a rare example of these species, Latos-Grażyński and co-workers reported that a cationic palladium(II) vacataporphyrin displayed a weak paratropic ring current ($\Delta\delta = 1.63$–2.67 ppm, nucleus-independent chemical shift (NICS): $+4.0$–6.0 ppm), which was ascribed to the 18π antiaromatic character based on the calculated Möbius structure, but without crystal structure evidence.[6] Thus, it can be said that structurally well-characterized Möbius antiaromatic species with a distinct paratropic ring current have not been reported to date.[7]

In general, the evaluation of aromaticity relies on energetic, geometric, and magnetic parameters. The most sensitive and widely applicable techniques for studying the magnetic properties are ^{1}H NMR chemical shifts, NICS,[8a] and anisotropy of the induced current density (AICD).[8b] In addition, our recent studies have demonstrated common photophysical properties for aromatic and antiaromatic porphyrinoids.[9] These antiaromatic expanded porphyrins exhibit several unique features that are not observed for their aromatic congeners: 1) broad and ill-defined absorption spectra without Q-like bands in the near-IR region, 2) weak or practically no fluorescence, 3) small two-photon absorption (TPA) cross-section values, and 4) very short excited-state lifetimes. These features are attributable to electronic features such as the relatively narrow HOMO–LUMO gap (HOMO = highest occupied molecular orbital, LUMO = lowest unoccupied molecular orbital) with perturbed degeneracy of HOMO/HOMO-1 and LUMO/LUMO + 1, and the presence of an optically forbidden S_1 state. These features are not observed for aromatic expanded porphyrins. Herein, we report a bisphosphorus complex of [30]hexaphyrin as the first example of a structurally well-characterized and stable $[4n+2]\pi$ Möbius antiaromatic molecule, in which the two incorporated phosphoramide moieties play important roles in rigidifying a singly twisted Möbius conformation and render a highly reduced [30]hexaphyrin stable.

Phosphorus insertion into porphyrinoids has proved a useful means to realize isophlorin-type fully reduced annulenic π conjugation.[10] Encouraged by these results, we attempted the reaction of meso-pentafluorophenyl [28]hexaphyrin(1.1.1.1.1.1) (**1a**) with $POCl_3$ (100 equiv) in the presence of triethylamine at room temperature for 24 h, which gave monophosphorus [28]hexaphyrin **2a** in 65 % yield after aqueous workup. We also found that a further treatment of **2a**

[*] J. M. Lim, J.-Y. Shin, Prof. Dr. D. Kim
Spectroscopy Laboratory for Functional π-electronic Systems and Department of Chemistry, Yonsei University
Seoul 120-749 (Korea)
Fax: (+82) 2-364-7050
E-mail: dongho@yonsei.ac.kr
T. Higashino, T. Miura, S. Saito, Prof. Dr. A. Osuka
Department of Chemistry
Graduate School of Science, Kyoto University
Sakyo-ku, Kyoto 606-8502 (Japan)
Fax: (+81) 75-753-3970
E-mail: osuka@kuchem.kyoto-u.ac.jp

[**] This work was supported by Grants-in-Aid (A) (No. 19205006 (A) and 20108001 "pi-Space") for Scientific Research from MEXT. The work at Yonsei University was supported by the Star Faculty and World Class University (R32-10217) programs from the Ministry of Education, Science, and Technology (MEST) of Korea and the AFSOR/AOARD grant (FA2386-09-1-4092). The AICD calculations were performed by using the supercomputing resource of the Korea Institute of Science and Technology Information (KISTI). S.S. acknowledges a JSPS Fellowship for Young Scientists. J.M.L acknowledges the Seoul Science Fellowship.

Supporting information for this article is available on the WWW under http://dx.doi.org/10.1002/anie.201001765.

with PCl_3 (50 equiv) in the presence of triethylamine at 0 °C for 1 h gave bisphosphorus [30]hexaphyrin **3a** in 46% yield. In the same manner, phosphorus complexes **2b** and **3b** were obtained from meso-(2,4,6-trifluorophenyl) substituted [28]hexaphyrin **1b** in 24 and 10% yield, respectively (Scheme 1).

Single-crystal X-ray diffraction analysis revealed a twisted Möbius structure of **2a**, in which a P=O moiety was bound to the β-carbon atom of the pyrrole unit C and the two nitrogen atoms of the pyrrole units A and B (Figure 1a).[11a] The ^{1}H NMR spectrum showed ten signals that correspond to the outer β protons in the range $\delta = 7.75$–6.53 ppm and a doublet at $\delta = 2.99$ ppm that corresponds to the inner β proton of the pyrrole unit C that was coupled to a phosphorus atom ($J =$ 6.9 Hz; Figure 2a and the Supporting Information). The assignment was confirmed by ^{1}H–^{1}H and ^{1}H–^{31}P NMR correlation measurements, and by the addition of D_2O (see the Supporting Information). Accordingly, the difference between the chemical shifts ($\Delta\delta$) of the most shielded and deshielded β protons was $\delta = 4.76$ ppm, thus indicating a moderate diatropic ring current despite the large dihedral angle (65°) along its π conjugation. The structural rigidity of **2a** in solution was indicated by virtually temperature-independent NMR spectra and only weak solvent-effects in the absorption spectra (see the Supporting Information), whereas **1a** exhibited dramatic temperature-dependent spectral changes.[5e] Accordingly, it can be concluded that **2a** is a normal Möbius aromatic molecule. The complex **2b** exhibited properties analogous to those of **2a**.

The structure of bisphosphorus complex **3a** was unambiguously determined by X-ray diffraction analysis to be a singly twisted Möbius conformation, in which the additionally embedded P=O moiety was bound to the three nitrogen atoms of the pyrrole units D, E, and F (Figure 1b).[11b] In addition, high-resolution ESI-TOF-MS and charge-balance considerations showed the complex **3a** was a reduced [30]hexaphyrin. This highly reduced molecule is probably stabilized by two strongly electron-withdrawing phosphoramide moieties. Interestingly, the ^{1}H NMR spectrum of **3a** revealed a remarkably deshielded doublet at $\delta = 11.14$ ppm that corresponds to the inner β proton of the pyrrole unit C, which was coupled with P^a ($J = 5.0$ Hz), ten signals that correspond to the outer β protons in a range of $\delta = 6.72$–5.54 ppm, and a relatively shielded broad singlet at $\delta =$ 7.15 ppm that correspond to the outer NH proton (Figure 2b and the Supporting Information). The observed apparent deshielding of the inner β proton and significant shielding of the outer β protons indicated a distinct paratropic ring current with $\Delta\delta = 5.60$ ppm. The observed moderate ring current may be ascribed to a large dihedral angle (66.8°) at the most distorted position. Complex **3b** displayed properties that are analogous to those of **3a**. The ^{1}H NMR analysis also indicated a moderate but distinct 30π Möbius antiaromaticity of **3b**. The most intriguing point here is that the shielding and deshielding effects of **2** and **3** are inverted only by changing the number of π electrons from [4*n*] to [4*n*+2], although their Möbius-type structures remain nearly the same. This observation suggests that the concept of Möbius aromaticity, which is a reversal of the Hückel rule, is valid for the expanded porphyrin systems.

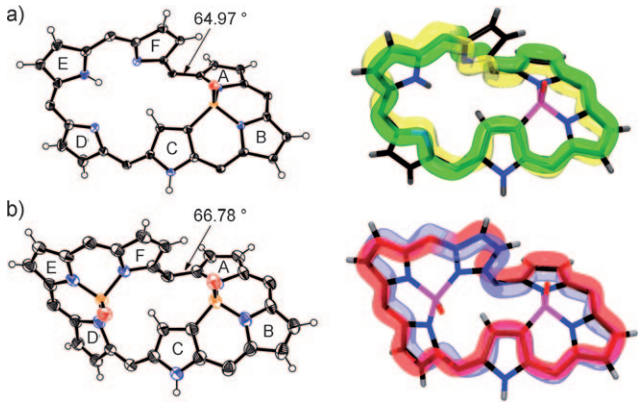

Figure 1. X-ray crystal structures (left) and schematic representations of molecular topologies (right) of a) **2a** and b) **3a**. Thermal ellipsoids represent 50% probability and meso-aryl substituents are omitted for clarity. Dihedral angles at the most distorted points are given.

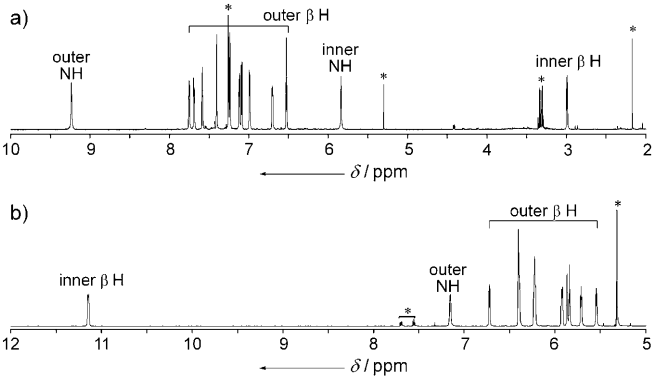

Figure 2. ^{1}H NMR spectra of a) **2a** in $CDCl_3$ and b) **3a** in CD_2Cl_2 at 25 °C. Peaks marked with a * arise from residual solvents and impurities.

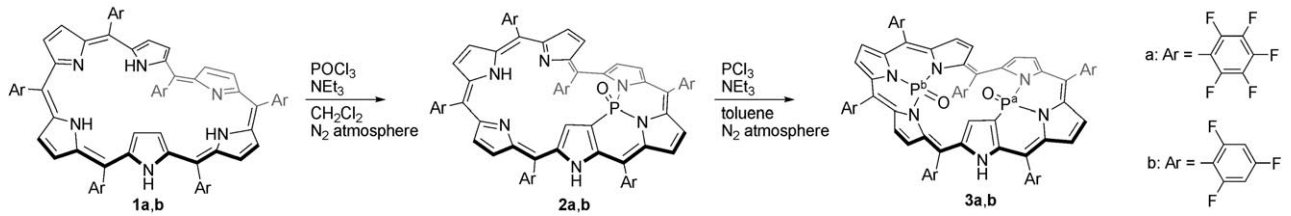

Scheme 1. Stepwise insertion of phosphorus into [28]hexaphyrins **1a** and **1b**.

In general, the absorption spectra of aromatic expanded porphyrins confirm a porphyrinlike structure, which is predicted by Gouterman's four orbital model.[12] As in the porphyrinoids, the four frontier molecular orbitals (MOs) of the aromatic expanded porphyrins, which consist of nearly degenerated HOMO/HOMO-1 and LUMO/LUMO + 1, participate in configuration interactions. The UV/Vis/NIR absorption spectrum of **2a** exhibits an intense B-like band at 588 nm and broad Q-like bands at 876 and 1055 nm (Figure 3). DFT calculations for **2a** show that the HOMO and

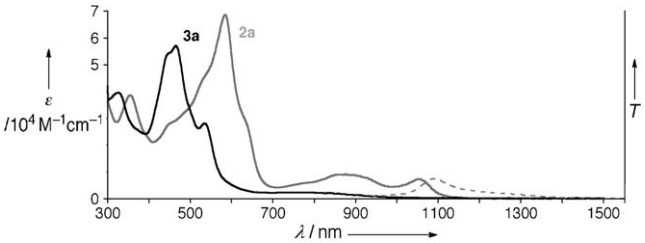

Figure 3. UV/Vis absorption spectra of **2a** (gray) and **3a** (black) in CH_2Cl_2. The fluorescence emission spectrum of **2a** is shown by a dotted line.

HOMO-1 are nearly degenerate, which is consistent with the absorption spectrum (see the Supporting Information). Moreover, **2a** exhibits a fluorescence band at 1090 nm, which is a mirror image of the corresponding absorption spectrum (Figure 3). In contrast, the UV/Vis/NIR absorption spectrum of **3a** shows ill-defined Soret-like bands and broad, weak NIR bands. Furthermore, **3a** shows no fluorescence emission (Figure 3). It should be noted that the absorption and fluorescence behavior of **3a** is similar to those of typical Hückel antiaromatic expanded porphyrins.[9a,b]

The aromaticity of expanded porphyrins is prominently distinguished in time-resolved and nonlinear optical (NLO) spectroscopic measurements. The Möbius aromatic molecule **2a** shows the distinct excited-state properties of aromatic expanded porphyrins. Typically, we have observed that the differential absorption spectra of aromatic expanded porphyrins show strong ground-state bleaching (GSB) signals with relatively weak excited-state absorption (ESA) signals. These signals are also seen in the transient absorption spectra of **2a** (Figure 4a). In contrast, the spectra of **3a** show small GSB and large ESA signals, and are quite different from those of **2a** (Figure 4b). These spectral features, together with faster decay dynamics of **3a** than **2a** (Figure 4), are unique for Hückel antiaromatic expanded porphyrins.[9a,b] The difference in excited-state dynamics between aromatic and antiaromatic expanded porphyrins could be mainly attributed to the different electronic structures of these two classes of molecules. The perturbed degeneracy of HOMO/HOMO-1 and LUMO/LUMO + 1 causes the interruption of two additional frontier MOs, thus resulting in a change in configuration interactions. As a consequence, the electronic transitions or states that affect the steady- and excited-state dynamics are perturbed. In fact, it was reported that a *trans*-vinylene-bridged antiaromatic hexaphyrin with MO structures similar to **3a** reveals the six frontier MOs mixing in time-dependent DFT (TD-DFT) calculations along with the same trend in the steady- and excited-state dynamics of **3a**, and the presence of the optical dark state governs its photophysical behavior.[9b] Based on these results, the fast decay of **3a** can be ascribed to the NIR dark state that acts as a ladder in the deactivation processes. The two-photon absorption (TPA) cross-section values of phosphorus hexaphyrins also exemplify the aromaticity difference between **2a** and **3a**. The aromatic **2a** shows a relatively large TPA cross-section value (3950 GM) compared to that of the antiaromatic **3a** (2400 GM; see the Supporting Information), which is also consistent with previous reports of the approximate proportionality between the degree of aromaticity and TPA values.[9c]

We performed DFT calculations (B3LYP/6-311G(d,p)) for **2a** and **3a** on the basis of both the crystal structure and the

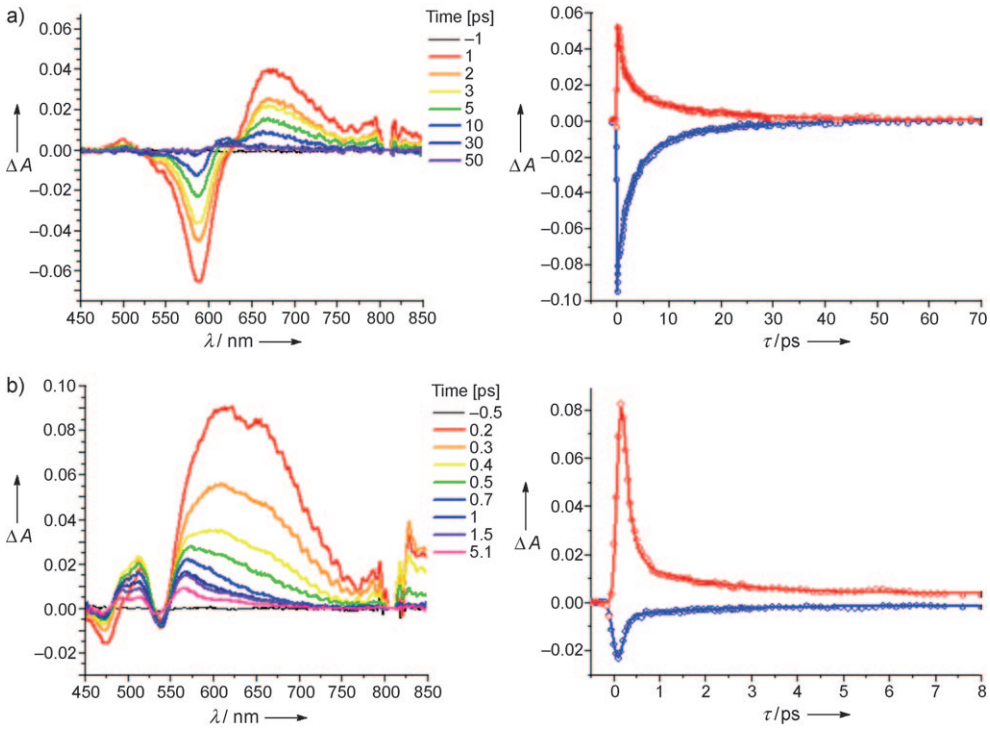

Figure 4. Femtosecond transient absorption spectra and decay profiles of a) **2a** and b) **3a**. The pump excitation is 585 nm for **2a** and 535 nm for **3a**. The decay profiles are observed at each maximum wavelength of bleaching and ESA signals.

optimized structures (see the Supporting Information).[13] Large negative NICS values were calculated at the center of **2a** ($\delta = -8.25$ ppm for the crystal structure and -11.99 ppm for the optimized structure) but small positive NICS values were calculated for **3a** ($\delta = +3.65$ ppm for the crystal structure and $\delta = +2.05$ ppm for the optimized structure); these values are consistent with the assignments of aromatic and antiaromatic character. In addition, we also attempted the direct visualization of the induced ring current.[8b] The AICD method is a powerful tool for the determination of the degree of aromaticity or antiaromaticity because it represents the 3D image of delocalized electron densities with a scalar field,[14] and is particularly useful for nonplanar π-conjugated systems such as **2a** and **3a**.Since the AICD plot illustrates the paramagnetic term of the induced current density, the aromatic molecules show clockwise current density and the antiaromatic species show counter-clockwise current density. The AICD plot of **2a** reveals clear clockwise current-density vectors, thus indicating a diamagnetic ring current (see the Supporting Information). On the contrary, the AICD plot of **3a** shows relatively weak counter-clockwise current flow, which implies an induced paratropic ring current. Furthermore, the AICD plots of **2a** and **3a** show a prominent difference upon changing the isosurface values (see the Supporting Information). Although **2a** shows a continuous boundary surface that encloses the delocalized electrons even at the isosurface value of 0.05, **3a** does not show a continuous current density above the isosurface value of 0.045. This difference between **2a** and **3a** indicates that π-electron conjugation is more facile in **2a**, which has a 28π-electronic distorted Möbius topology, compared with **3a**, which has a 30π-electronic circuit. These results demonstrate that **2a** has a Möbius aromatic character with continuous and diamagnetic current density in its distorted conformation and that, more importantly, the Möbius antiaromaticity of **3a** is confirmed by a 3D paratropic ring current in spite of a weak density of delocalized electrons.

The electrochemical properties were studied by cyclic voltammetry in CH_2Cl_2 versus ferrocene/ferrocenium (Fc/Fc^+) with tetrabutylammonium hexafluorophosphate as electrolyte. Complex **2a** underwent two reversible oxidations at 0.46 and 0.84 V and two reversible reductions at -0.73 and -1.05 V, while **3a** showed two reversible oxidations at 0.12 and 0.27 V and two irreversible reductions around -1.41 and -1.86 V. The highly reduced hexaphyrin **3a** exhibited an elevated HOMO and resistance toward reduction.

In summary, the monophosphorus complexes of [28]hexaphyrins and bisphosphorus complexes of [30]hexaphyrins have been synthesized and characterized as $[4n]\pi$ Möbius aromatic and $[4n+2]\pi$ Möbius antiaromatic compounds, respectively. The twisted Möbius structures were confirmed by single-crystal X-ray diffraction analysis. The aromaticity and antiaromaticity was investigated by examining magnetic environments (^{1}H NMR chemical shifts, NICS, and induced current density maps) and the photophysical properties (UV/Vis/NIR absorption, singlet excited-state dynamics, NLO properties, and quantum mechanical calculations). Bisphosphorus [30]hexaphyrins have been determined to be the first structurally characterized Möbius antiaromatic systems, which are stable, neutral, and rigid. In this system, the phosphoramide moieties help maintain the distorted Möbius structure and, at the same time, stabilize the highly reduced 30π-electron state by their inductive electron-withdrawing effect. In this work, the aromaticity reversal in the Hückel rule upon changing the number of π electrons between $[4n+2]$ and $[4n]$ has been validated also for cyclic conjugated molecules with a twisted Möbius topology.

Received: March 25, 2010
Published online: June 2, 2010

Keywords: aromaticity · hexaphyrins · Möbius aromaticity · phosphorus · porphyrinoids

[1] a) H. E. Zimmerman, *Acc. Chem. Res.* **1971**, *4*, 272 – 280; b) H. S. Rzepa, *Chem. Rev.* **2005**, *105*, 3697 – 3715; c) R. Herges, *Chem. Rev.* **2006**, *106*, 4820 – 4842.

[2] E. Heilbronner, *Tetrahedron Lett.* **1964**, *5*, 1923 – 1928.

[3] M. Mauksch, V. Gogonea, H. Jiao, P. v. R. Schleyer, *Angew. Chem.* **1998**, *110*, 2515 – 2517; *Angew. Chem. Int. Ed.* **1998**, *37*, 2395 – 2397.

[4] a) D. Ajami, O. Oeckler, A. Simon, R. Herges, *Nature* **2003**, *426*, 819 – 821; b) C. Castro, Z. Chen, C. S. Wannere, H. Jiao, W. L. Karney, M. Mauksch, R. Puchta, N. J. R. v. E. Hommes, P. v. R. Schleyer, *J. Am. Chem. Soc.* **2005**, *127*, 2425 – 2432; c) D. Ajami, K. Hess, F. Köhler, C. Näther, O. Oeckler, A. Simon, C. Yamamoto, Y. Okamoto, R. Herges, *Chem. Eur. J.* **2006**, *12*, 5434 – 5445.

[5] a) M. Stępień, L. Latos-Grażyński, N. Sprutta, P. Chwalisz, L. Szterenberg, *Angew. Chem.* **2007**, *119*, 8015 – 8019; *Angew. Chem. Int. Ed.* **2007**, *46*, 7869 – 7873; b) Z. S. Yoon, A. Osuka, D. Kim, *Nat. Chem.* **2009**, *1*, 113 – 122; c) Y. Tanaka, S. Saito, S. Mori, N. Aratani, H. Shinokubo, N. Shibata, Y. Higuchi, Z. S. Yoon, K. S. Kim, S. B. Noh, J. K. Park, D. Kim, A. Osuka, *Angew. Chem.* **2008**, *120*, 693 – 696; *Angew. Chem. Int. Ed.* **2008**, *47*, 681 – 684; d) J. K. Park, Z. S. Yoon, M.-C. Yoon, K. S. Kim, S. Mori, J.-Y. Shin, A. Osuka, D. Kim, *J. Am. Chem. Soc.* **2008**, *130*, 1824 – 1825; e) J. Sankar, S. Mori, S. Saito, H. Rath, M. Suzuki, Y. Inokuma, H. Shinokubo, K. S. Kim, Z. S. Yoon, J.-Y. Shin, J. M. Lim, Y. Matsuzaki, O. Matsushita, A. Muranaka, N. Kobayashi, D. Kim, A. Osuka, *J. Am. Chem. Soc.* **2008**, *130*, 13568 – 13579; f) S. Saito, J.-Y. Shin, J. M. Lim, K. S. Kim, D. Kim, A. Osuka, *Angew. Chem.* **2008**, *120*, 9803 – 9806; *Angew. Chem. Int. Ed.* **2008**, *47*, 9657 – 9660; g) S. Tokuji, J.-Y. Shin, K. S. Kim, J. M. Lim, K. Youfu, S. Saito, D. Kim, A. Osuka, *J. Am. Chem. Soc.* **2009**, *131*, 7240 – 7241.

[6] E. Pacholska-Dudziak, J. Skonieczny, M. Pawlicki, L. Szterenberg, Z. Ciunik, L. Latos-Grażyński, *J. Am. Chem. Soc.* **2008**, *130*, 6182 – 6195.

[7] a) P. M. Warner, *J. Org. Chem.* **2006**, *71*, 9271 – 9282; b) K. B. Wiberg, *Chem. Rev.* **2001**, *101*, 1317 – 1331.

[8] a) P. v. R. Schleyer, C. Maerker, A. Dransfeld, H. Jiao, N. J. R. v. E. Hommes, *J. Am. Chem. Soc.* **1996**, *118*, 6317 – 6318; b) D. Geuenich, K. Hess, F. Köhler, R. Herges, *Chem. Rev.* **2005**, *105*, 3758 – 3772.

[9] a) S. Mori, K. S. Kim, Z. S. Yoon, S. B. Noh, D. Kim, A. Osuka, *J. Am. Chem. Soc.* **2007**, *129*, 11344 – 11345; b) M.-C. Yoon, S. Cho, M. Suzuki, A. Osuka, D. Kim, *J. Am. Chem. Soc.* **2009**, *131*, 7360 – 7367; c) J. M. Lim, Z. S. Yoon, J.-Y. Shin, K. S. Kim, M.-C. Yoon, D. Kim, *Chem. Commun.* **2009**, 261 – 273; d) J. M. Lim, J.-Y. Shin, Y. Tanaka, S. Saito, A. Osuka, D. Kim, *J. Am. Chem. Soc.* **2010**, *132*, 3105 – 3114.

[10] a) A. Młodzianowska, L. Latos-Grażyński, L. Szterenberg, *Inorg. Chem.* **2008**, *47*, 6364 – 6374; b) E. Pacholska-Dudziak, F. Ulatowski, Z. Ciunik, L. Latos-Grażyński, *Chem. Eur. J.* **2009**, *15*, 10924 – 10929; c) T. Miura, T. Higashino, S. Saito, A. Osuka, *Chem. Eur. J.* **2010**, *16*, 55 – 59.

[11] a) Crystallographic data for **2a**: $C_{199}H_{90}F_{60}N_{12}O_2P_2$, $M_r = 3882.77$; monoclinic; space group $P2_1/c$ (No.14), $a = 14.6459(18)$, $b = 40.056(5)$, $c = 14.0843(18)$ Å; $\beta = 90.871(2)°$; $V = 8261.8(18)$ Å^3; $\rho_{calcd} = 1.561$ g cm^{-3}; $Z = 2$; $R_1 = 0.0763$ [$I > 2.0\sigma(I)$], $wR_2 = 0.1972$ (all data), GOF = 1.067; b) Crystallographic data for **3a**: $C_{84}H_{48}F_{30}N_6O_8P_2$, $M_r = 1901.22$; monoclinic; space group $P2_1/n$ (No.14), $a = 18.458(6)$, $b = 16.429(4)$, $c = 26.966(9)$ Å; $\beta = 91.314(11)°$; $V = 8175(4)$ Å^3; $\rho_{calcd} = 1.545$ g cm^{-3}; $Z = 4$; $R_1 = 0.0995$ [$I > 2.0\sigma(I)$], $wR_2 = 0.3005$ (all data), GOF = 1.046. CCDC-760748(**2a**), and 760749 (**3a**) contain the supplementary crystallographic data for this paper. These data can be obtained free of charge from The Cambridge Crystallographic Data Centre via www.ccdc.cam.ac.uk/data_request/cif.

[12] a) T. K. Ahn, J. H. Kwon, D. Y. Kim, D. W. Cho, D. H. Jeong, S. K. Kim, M. Suzuki, S. Shimizu, A. Osuka, D. Kim, *J. Am. Chem. Soc.* **2005**, *127*, 12856 – 12861; b) J.-Y. Shin, J. M. Lim, Z. S. Yoon, K. S. Kim, M.-C. Yoon, S. Hiroto, H. Shinokubo, S. Shimizu, A. Osuka, D. Kim, *J. Phys. Chem. B* **2009**, *113*, 5794 – 5802.

[13] M. J. Frisch, et al. *Gaussian 09*, revision A.02; Gaussian, Inc.: Wallingford, CT, **2009**.

[14] a) E. Steiner, P. W. Fowler, *Org. Biomol. Chem.* **2006**, *4*, 2473 – 2476; b) E.-U. Wallenborn, R. F. Haldimann, F.-G. Klärner, F. Diederich, *Chem. Eur. J.* **1998**, *4*, 2258 – 2265.

